

## Extracellular Synthesis of Iron Oxide NPs by Using Several Bacteria Genera Isolated from Oil Contaminated Sites in Basrah Governorate

Hawraa Qays Al-assdy<sup>1</sup>, Wijdan Hussein Al-Tamimi<sup>1</sup>, Asia Fadhile Almansoor<sup>2</sup>

<sup>1</sup>Department of Biology College of Science, University of Basrah, Iraq

<sup>2</sup>Department of Ecology, College of Science, University of Basrah, Iraq

\*Corresponding Author: [hawraa.qais@uobasrah.edu.iq](mailto:hawraa.qais@uobasrah.edu.iq)

### ARTICLE INFO

#### Article History:

Received: July 24, 2024

Accepted: Aug. 11, 2024

Online: Aug. 21, 2024

#### Keywords:

16srDNA sequencing,  
Synthesized IONPs,  
Contaminated sites,  
Basrah Governorate

### ABSTRACT

Nanotechnology is a developing field of research that focuses on manipulating the structure of matter at the atomic and molecular level. Twenty-two bacterial isolates were isolated from five contaminant sites of wastewater, sludge, and soil in Basrah Governorate. The isolates were identified by 16S rRNA gene sequencing analysis. The isolated bacteria was investigated to reduce nitrate and screen for production of iron oxide nanoparticles (IONPs) by determining the weight of yield for each isolate, and measuring the absorbance by using UV-Vis spectrophotometer. The results of genetic identification showed that bacterial isolates belonged to the genera of *Alishewanella*, *Stutzerimonas*, *Mixta*, *Pantoea*, *Leclercia*, *Citrobacter*, *Bacillus*, *Franconibacter*, *Enterobacter*, *Shigella*, *Lysinibacillus*, *Halotalea*, and *Enterobacteriaceae*. Depending on the 16S rDNA gene sequences, the phylogenetic tree was built to show the evolutionary relationships between the isolated bacteria. Nine new strains were recorded in the GenBank. All bacterial isolates were positive to nitrate reduction test and the color of the medium changed from pale yellow to brown or reddish brown indicating the reduction of iron salt  $FeCl_3 \cdot 6H_2O$  to IONPs, moreover the range of absorbance was between 342–457nm. The weight of IONPs synthesis ranged from 0.02 to 0.702g/ l. *Alishewanella jeotgali* KCTC 22429, *Leclercia adecarboxylata* strain V894, and *Lysinibacillus boronitolerans* strain Mix24 achieved the highest rate of production of IONPs 0.702, 0.5 and 0.46g/ l, respectively. The abundance of diverse bacteria suggests that they possess an inherent ability to function as viable bio factories in the creation of nanoparticles.

### INTRODUCTION

The petroleum refinery effluents are generated as a result of the crude oil processing. It consists of hazardous substances, including heavy metals, polycyclic aromatic hydrocarbons (PAHs), and total petroleum hydrocarbons (TPH) (Almutairi, 2024). The conditions such as high pressure, high temperatures, high salt content, and little water activity in oil field reservoirs, prevent many bacteria to survive there (Pannekens *et al.*, 2019). Several significant bacterial species were isolated and identified in oil-contaminated soil that have the ability to biodegrade petroleum. These species include *Vibrio Xanthomonas*, *Bacillus* sp., *Aeromonas* sp., *Acinetobacter* sp.,

*Flavobacterium* sp., *Micrococcus* sp., *Staphylococcus* sp., and *Pseudomonas* sp. (**Abdul-Ameer, 2019**).

Nanotechnology is an important field of research that focuses on supramolecular level, namely within the range of 1 to 100 nanometers. This manipulation is done to create specific qualities and functionalities, as well as for various applications (**Elfeky *et al.*, 2020**). Metal oxide nanoparticles have garnered significant interest as a result of their distinct and atypical physical and chemical characteristics (**Alhalili, 2023**). Metal oxide nanoparticles are highly significant due to their crucial involvement in various domains, including information technology, material chemistry, biomedical sciences, medicine, agriculture, electronics, optics, catalysis, environmental studies, and energy research (**Ene *et al.*, 2020**). Reducing the dimensions of nanoparticles enhances their surface area, modifies their magnetic, chemical, and electrical properties, and alters the features of metal oxide nanoparticles (**Ahmad *et al.*, 2022**).

Iron oxide nanoparticles (IONPs), a type of metal oxide nanoparticles, exhibit many shapes and possess distinct features (**Üstün *et al.*, 2022**). Iron can be found in several forms, including wustite (FeO), maghemite ( $\gamma$ -Fe<sub>2</sub>O<sub>3</sub>), magnetite (Fe<sub>3</sub>O<sub>4</sub>), and hematite ( $\alpha$ -Fe<sub>2</sub>O<sub>3</sub>). In addition, the presence of greigite (Fe<sub>3</sub>S<sub>4</sub>), ferrihydrite (Fe<sub>5</sub>OH<sub>8</sub>x4H<sub>2</sub>O), akaganeite ( $\beta$ -FeOOH), goethite ( $\alpha$ -FeOOH), and lepidocrocite ( $\gamma$ -FeOOH) has been detected. Magnetite, hematite, maghemite, and greigite exhibit ferrimagnetic qualities, while ferrihydrite, wustite, and goethite display antiferromagnetic traits. Akaganeite nanocrystals exhibit low magnetic properties. Out of all the other types, only magnetite and maghemite nanoparticles possess useful properties (**Gorobets *et al.*, 2017**).

Iron oxide nanoparticles may be produced using many methods, including sonochemical reactions, thermal decomposition, hydrothermal applications and biological methods (**Nadeem *et al.*, 2021**; **Samrot *et al.*, 2021**). Biological approaches for synthesized metal and metal oxides are considered the most desirable due to their safety, cost-effectiveness, and straightforward synthesis methodology (**Shafey, 2020**). The production of IONPs by biological processes may be classified into two main categories. The first category includes the use of microorganisms, including algae, bacteria, and fungi, as reducing agents. The second category is using plant extracts as both reduction and stabilization agents (**Salem *et al.*, 2019**; **Yew *et al.*, 2020**). The utilization of microorganisms for the synthesis of IONPs has garnered significant interest in recent decades due to its benefits over traditional physical and chemical synthesis methods. These benefits include the plentiful availability of microorganisms, the creation of less harmful byproducts, the consumption of lower amounts of power and energy due to synthesis occurring at room temperature, and the ability to handle large-scale manufacturing (**Park *et al.*, 2016**). Bacteria have been used to produce IONPs via extracellular or intracellular processes.

The intracellular mechanism entails the enzyme-mediated reduction of metal ions or metal oxide ions by electrostatically attaching them to the cell wall of microorganisms.

The ions then permeate into the cell and interact with enzymes, resulting in the formation of IONPs (Mukherjee, 2017). The extracellular method involves the enzymatic reduction of iron ions, resulting in the formation of nanoparticles (NPs) that have a tiny size distribution and are well disseminated. These NPs are stabilized and prevented from clumping together by genes, peptides, or proteins that act as reducing agents (Singh *et al.*, 2016). The biosynthesis of IONPs using bacterial supernatant such as *B. circulans*, *E. coli*, *Lactobacillus fermentum*, *B. subtilis*, *B. cereus*, and *Pseudomonas aeruginosa* which is considered a cost-effective and environmentally friendly alternative to conventional synthesis methods (Sundaram *et al.*, 2012; Crespo *et al.*, 2017; Fatemi *et al.*, 2018; Fani *et al.*, 2018; Hassan & Mahmood, 2019; Rabani *et al.*, 2023). Therefore, this study aimed to investigate the bacterial diversity in different contaminated sites aligned with screening the bacteria for the synthesized iron oxide nanoparticles.

## MATERIALS AND METHODS

### 2. Sample collection

Seven samples were collected from various contaminated environments, including wastewater, soil, and sludge. These samples were taken from the Al-Shuaiba Refinery, as well as from the washing and lubrication station in Zubair, Qurna, and Jazira. Additionally, soil samples were collected from the beach in Qurna. The sampling period spanned three months, from November 2022 to January 2023, as shown in Table (1). The five sampling locations are depicted in Fig. (1). Soil samples were collected at a depth of 5cm using a sterile spatula and transferred to sterile containers. Sludge and 500ml wastewater samples from the remediation basins at Al-Shuaiba Refinery were collected using sterile containers. All samples were then transported to the laboratory for examination.

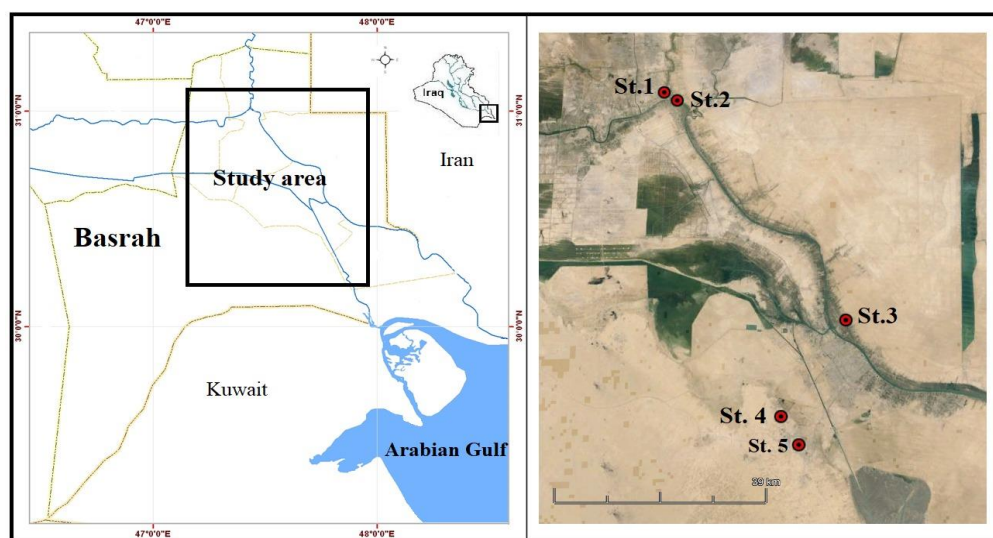


**Fig. 1.** Map showing study sites and samples sites from Basrah Governorate, southern Iraq

**Table 1.** Site of samples collection

Code of location	Name of location	Type of sample
HA	Remediation basins of Al-Shuaiba Refinery	wastewater
HB	Al-Shuaiba Refinery	Soil
HC	Al-Shuaiba Refinery	sludge
HD	Washing and lubrication station of Zubair	Soil
HE	Beach of Shatt Al -Arab	Soil
HF	Washing and lubrication station of Qurna	Soil
HR	Washing and lubrication station of Jazira	Soil

## 2. Isolation of bacteria

One milliliter of wastewater sample was mixed with nine milliliters of sterile distilled water, and further diluted to a concentration of  $10^{-5}$ . The mixture was then spread out onto nutrient and MacConkey agar plates and incubated at 37°C for 24h. One gram of soil and sludge samples were activated with 100ml of nutrient broth, and shaken for 1h, then diluted to a  $10^{-7}$  concentration and cultured according to the previous steps. In order to get pure isolates, the various samples were recultured on a nutrient agar using streaking methods. The bacterial isolates were checked for purity by Gram staining, then maintained on nutrient agar slants.

## 3. Molecular identification of bacterial isolates

### *DNA extraction and PCR amplification*

The extraction of the DNA from the bacteria was employed according to instruction Presto™ Mini g DNA bacteria kit (Geneaid, Taiwan). The 16S rDNA gene was amplified by PCR using universal primers 27F (5-AGAGTTTGATCCTGGCTCAG3) and 1492R (5- GGTTACCTTGTTACGACTT-3). In order to amplify the target 16S rDNA gene, the PCR procedure involved denaturation at 96°C for 3 minutes, followed by 27 cycles of denaturation at 96°C for 30s, annealing at 56°C for 25 seconds, elongation at 72°C for 15 seconds, and lastly, elongation at 72°C for 10 minutes. The PCR products were measured using gel electrophoresis, and a UV transilluminator was used to visualize and capture photos of them alongside a DNA ladder (Intronbio, South Korea) serving as a marker (Miyoshi *et al.*, 2005).

### 4. Identification of bacterial isolates and analysis the sequence data

The PCR product purification and sequencing was made in MacroGen Company (South Korea). The chromas were used for the purpose of proofreading the acquired 16S

rDNA gene sequences. The bacterial species were identified by Basic Local Alignment search tool (BLAST) that belongs to the National Center for Biotechnology Information (NCBI)“<http://www.ncbi.nlm.nih.gov>”.The sequence results were copied and pasted in the “BLAST”, then the program identified the bacterial species by comparing and aligning their sequences with nucleotide sequences databases of NCBI. Additionally, the phylogenetic tree was constructed using MEGA X (Kumar *et al.*, 2018).

## 5. Screening isolates for extracellular biosynthesis of IONP

### 1. Nitrate reductase test

The nitrate reductase test was achieved as described by Bhusal and Muriana (2021).

### 2. The alterations in the color of mixture

The bacterial inoculum was prepared by activating bacteria in nutrient broth, which was then incubated in a shaking incubator at 150rpm and 37°C for 24 hours. After activation, 5% of the culture was used to inoculate 100ml of fresh nutrient broth, which was also incubated at 150rpm and 37°C for 24 hours. Following incubation, the bacterial culture was centrifuged at 4,000rpm for 10 minutes. The supernatant was transferred to a new flask and used for the synthesis of iron oxide nanoparticles (IONPs). A 2mM FeCl<sub>3</sub>·6H<sub>2</sub>O solution was mixed with the bacterial supernatant in a 1:1 ratio and incubated at 150rpm and 37°C for 2 days. The color of the supernatant was visually monitored for any changes during IONP production. A color change from light yellow to brown or reddish brown indicated a positive result.

### 3. Measurement of light absorption in bacterial culture supernatants

Following the incubation duration, in order to check the presence of IONPs in supernatant of various strains, each reaction mixture that became dark or reddish-brown had two milliliters removed and put into quartz cuvettes. The absorbance in the 200–800nm region was measured using the Dual Beam UV–Vis 1900 Spectrophotometer apparatus (Shimadzu, Japan) (Valentina, 2022).

### 4. Weight of the synthesized IONPs

After measuring the absorbance, the samples were subjected to centrifugation at a speed of 10000rpm per minute for a duration of 10 minutes using a centrifuge (Gemmy, Taiwan). The liquid portion above the sediment, known as the supernatant, was then discarded. The next step included dispersing the IONPs, or iron oxide nanoparticles, using deionized water. This procedure was conducted on three separate occasions. The purified precipitates were desiccated by exposure to ambient air, then collected in the form of powder, and measured in terms of weight (Singh *et al.*, 2018).

## RESULTS

The results showed that a total of twenty -two pure bacterial isolates were obtained in the current study, five pure bacterial isolates from wastewater (HA) and soil (HB), one from sludge (HC) and soil (HE), four from soil (HD) and (HF) and two from soil (HR). The results of the Gram- staining procedure indicated that 77.3% of bacterial isolates were Gram- negative, and 22.7% were Gram- positive, as shown in Fig. (2). Gram staining revealed that 100% of bacteria isolated were Gram- negative in wastewater (HA), sludge (HC), soil (HD), and soil (HR), whereas samples of soil (HB), (HE), and (HF) were 20% Gram- positive and 80% Gram- negative, 100% (Gram -positive), and 75% (Gram -positive), and 25% (Gram – negative), respectively.

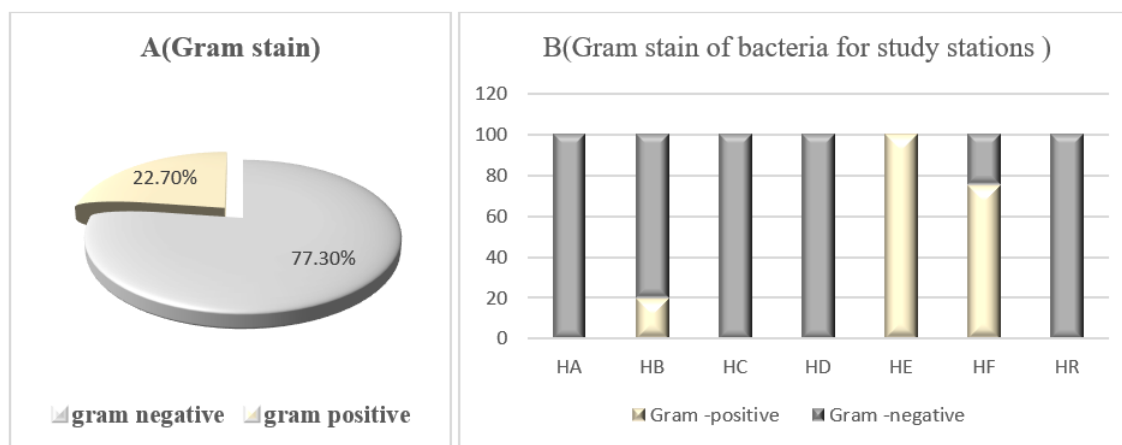


**Fig. 2. (A)** Total percentage of Gram- positive and Gram-negative bacteria at all stations; **(B)** Gram staining of bacteria at different study stations

### 1. Identification of bacterial isolates by 16S rDNA gene sequencing

The electrophoresis of the 16S rDNA gene PCR findings for all bacterial isolates was seen using a UV transilluminator. The gene was located at about 1500 base pairs, as shown by the DNA ladder in Fig. (3). The BLAST software was used to scrutinize and align the DNA sequencing outcomes of isolates with their corresponding reference strains in the GenBank .After alignment with other 16S rDNA sequences, the degree of similarity of isolates was 96.39– 100% to references strain. The 16S rDNA gene sequencing of all bacterial isolates revealed that the isolates belong to 13 different genera, as shown in Table (2). They belong to *Alishewanella*, *Stutzerimonas*, *Mixta*, *Pantoea*, *Leclercia citrobacter*, *Bacillus*, *Franconibacter*, *Enterobacter*, *Shigella*, *Lysinibacillus*, *Halotalea*, and *Enterobacteriaceae*.

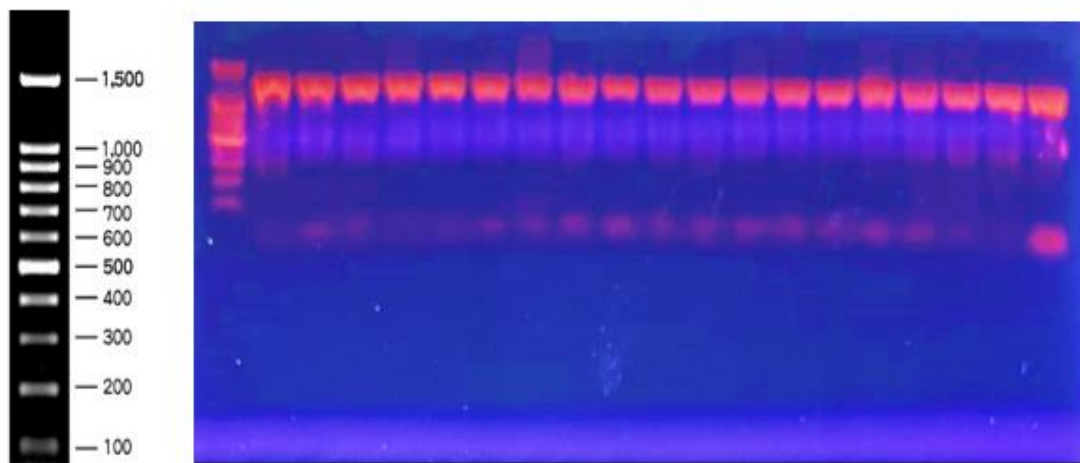


**Fig. 3.** The electrophoresis of the 16S rDNA gene reveals the presence of amplified genomic DNA obtained from bacteria

**Table 2.** Identification of bacterial isolates by 16SrDNA gene sequences

Samples	Isolates code	Closest specie	Identity %	Accession no.
HA	HA5	<i>Alishewanella fetalis</i> strain KD 167	99.93%	MN809397
	HA6	<i>Stutzerimonas stutzeri</i> strain Xmb018	99.93%	KT986148
	HA7	<i>Alishewanella agri</i> strain ZJY-583	99.35%	KP282808
	HA8	<i>Stutzerimonas stutzeri</i> strain WAB2185	100%	MH169303
	HA9	<i>Stutzerimonas stutzeri</i> strain IRQNWYF2	100%	MT261835
HB	HB4	<i>Mixta theicola</i> strain SSK_C8	99.93%	MZ357957
	HB5	<i>Pantoea alhagi</i>	100%	MW296119
	HB6	<i>Leclercia adecarboxylata</i> strain V894	99.91%	OR431468
	HB7	<i>Citrobacter sedlakii</i> strain Remi_14	100%	MT507093
	HB8	<i>Bacillus paramycoides</i> strain 3664	100%	MT538528
HC	HC3	<i>Alishewanella jeotgali</i> KCTC 22429	99.35%	NR_116459
HD	HD3	<i>Franconibacter daqui</i> strain L17	100%	OK509193
	HD4	<i>Enterobacter hormaechei</i> strain WG12L-2G-A	100%	OP288194
	HD5	<i>Shigella sonnei</i> strain 08BF03TD	100%	KX146471

	HD6	<i>Enterobacteriaceae bacterium v450</i>	100%	EF088377
HE	HE2	<i>Lysinibacillus boronitolerans strain Mix24</i>	100%	MH385002
	HF2	<i>Bacillus cereus strain SPA1.1</i>	99.91%	MK694742
	HF3	<i>Lysinibacillus macroides strain SKC-16</i>	100%	MT218365
HF	HF4	<i>Lysinibacillus boronitolerans strain Mix24</i>	100%	MH385002
	HF5	<i>Halotalea alkalilenta strain AW-7</i>	96.39%	NR_043806
	HR2	<i>Enterobacter cloacae strain UKME01</i>	100%	KX266259
HR	HR3	<i>Enterobacteriaceae bacterium v450</i>	99.72%	EF088377

Out of 22 isolates, 9 isolates were recorded as new strains and deposited to the GenBank database under the accession numbers (OR885474, OR890431, OR885475, OR885469, OR885470, OR885471, OR890436, OR957372, and OR957409), as shown in Table (3).

**Table 3.** The bacterial isolates characterized as new bacterial strains

Samples	Isolates code	New bacterial strains	Identity %	Accession no. of new strain
	HA5	<i>Alishewanella fetalis strain HAQ12</i>	99.93%	OR885474
HA	HA6	<i>Stutzerimonas stutzeri strain HAQ13</i>	99.93%	OR890431
	HA7	<i>Alishewanella agri strain HAQ15</i>	99.35%	OR885475
	HB4	<i>Mixta theicola strain HAQ</i>	99.93%	OR885469
HB	HB6	<i>Leclercia adecarboxylata strain HAQ</i>	99.91%	OR885470
HC	HC3	<i>Alishewanella jeotgali strain HAQ8</i>	99.35%	OR885471
	HF2	<i>Bacillus cereus strain HAQ35</i>	99.91%	OR890436
HF	HF5	<i>Halotalea alkalilenta strain HAQ28</i>	96.39%	OR957372
	HR3	<i>Enterobacteriaceae bacterium strain HAQ24</i>	99.72%	OR957409

The phylogenetic tree, depicted in Fig. (4), illustrates the relationships between the 22 different bacterial isolates that were isolated from different contaminated sites.



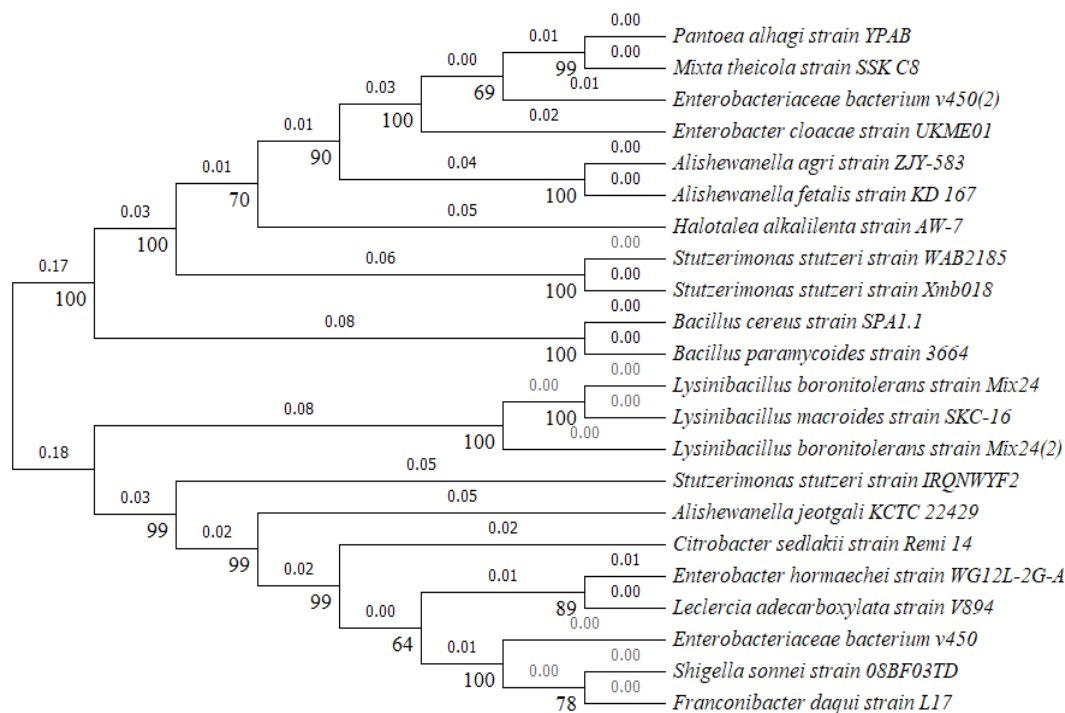


**Fig. 4.** The NJ method of phylogenetic tree construction illustrating the evolutionary relationships among bacterial isolates

#### Bacterial screening for the ability to synthesize IONPs

All isolated bacteria were selected to test their ability for the synthesis of IONPs, as shown in Table (4). The result of nitrate reduction test showed that all isolates were positive (Fig. 5).



**Fig. 5.** The final results of the nitrate reductase enzyme test

The results of the synthesis of IONPs showed that all mixtures color (supernatant and  $\text{FeCl}_3 \cdot 6\text{H}_2\text{O}$ ) changed from pale yellow to brown or reddish brown indicating a successful synthesis of IONPs, as shown in Fig. (6). The nanoparticles synthesized was confirmed by measuring of UV-vis absorption spectroscopy within the wavelength range

of 200 to 800nm. The absorption bands have been ranged between 342–457nm, as shown in Fig. (7) and Table (4).

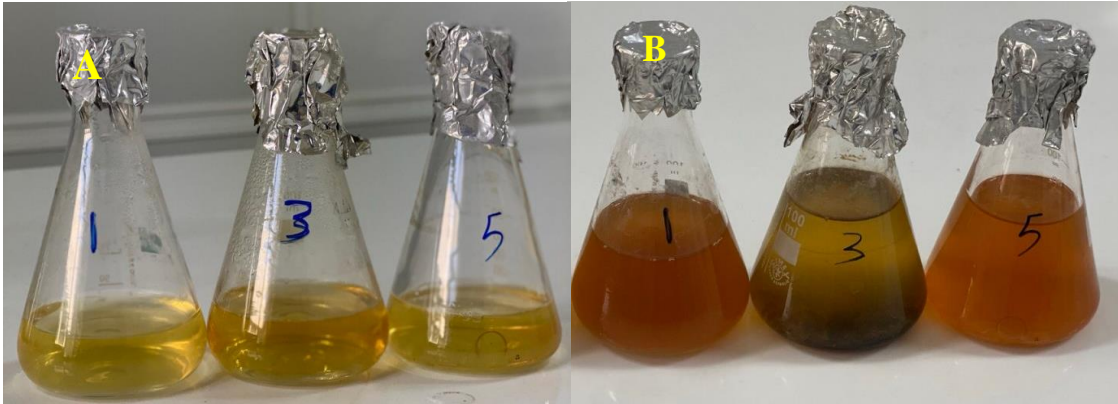


**Fig. 6.** The color change of mixture. **A:** bacteria superntant. **B:** bacteria superntant interaction with iron salt and result in change mixture color and synthesis IONPs

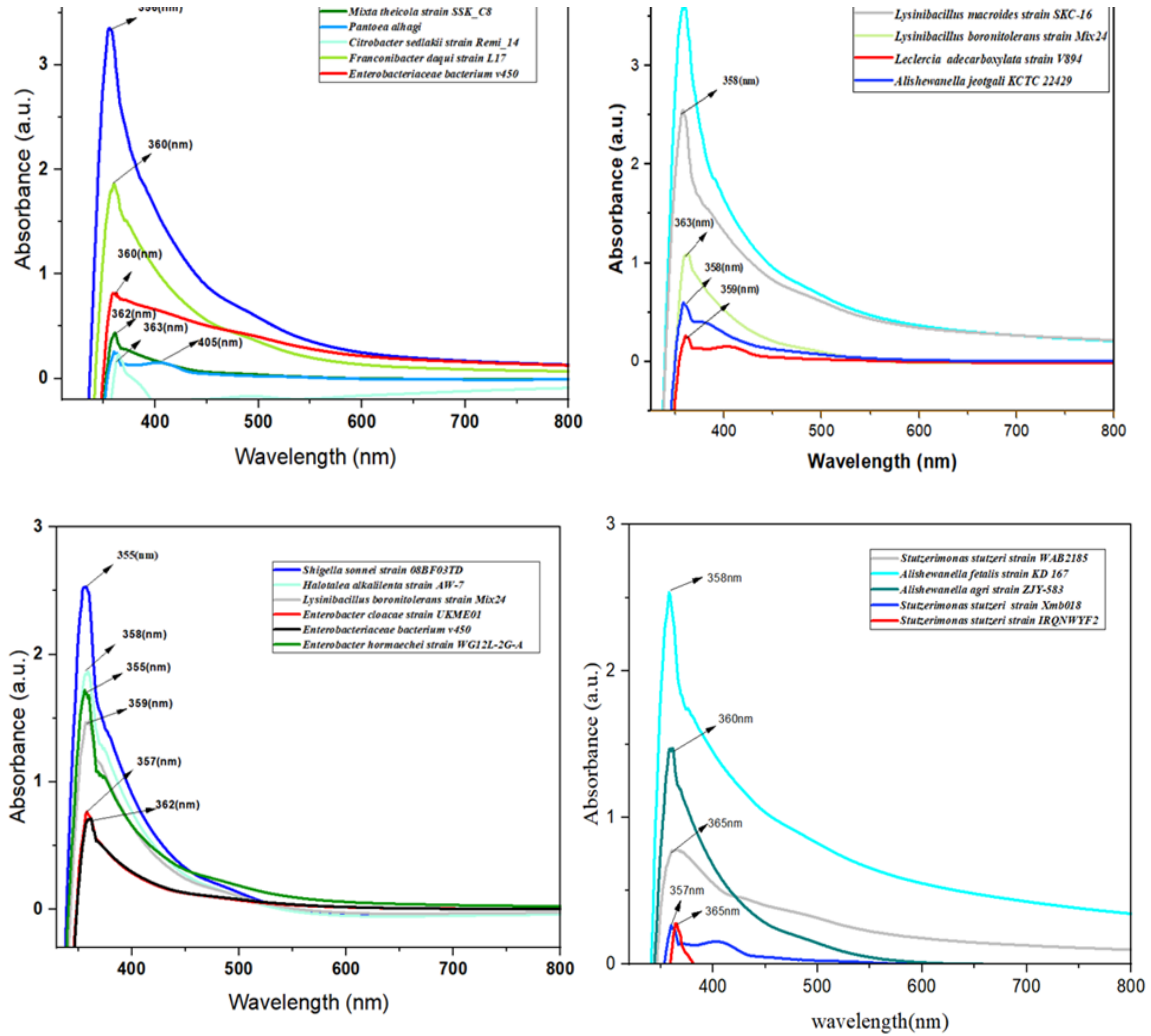


**Fig. 7.** UV–vis spectra of IONPs produced by 22 different bacterial strains in their supernatant

The results of screening of bacterial isolates according to the weight of IONPs synthesized showed that the yield weight ranged between 0.02 and 0.702g /l. The three isolates *Alishewanella jeotgali* KCTC 22429, *Leclercia adecarboxylata* strain V894 and *Lysinibacillus boronitolerans* strain Mix24 were superior, and the highest rate of production was 0.702, 0.5, and 0.46g/ l, respectively, as depicted in Table (4).

**Table 4.** Results of the bacterial screening for the biosynthesis of IONPs

Code of sample	Bacteria isolate	NR Enzyme	wavelength nm	Absorption	weight g/l
HA5	<i>Alishewanella fetalis</i> strain KD 167	+	358	2.528	0.26
HA6	<i>Stutzerimonas stutzeri</i> strain Xmb018	+	457	0.101	0.372
HA7	<i>Alishewanella agri</i> strain ZJY-583	+	360	0.25	0.28
HA8	<i>Stutzerimonas stutzeri</i> strain WAB2185	+	369	0.775	0.02
HA9	<i>Stutzerimonas stutzeri</i> strain IRQNWYF2	+	365	0.272	0.17
HB4	<i>Mixta theicola</i> strain SSK_C8	+	362	0.420	0.38
HB5	<i>Pantoea alhagi</i>	+	405	0.160	0.324
HB6	<i>Leclercia adecarboxylata</i> strain V894	+	359	0.244	0.5
HB7	<i>Citrobacter sedlakii</i> strain Remi_14	+	363	0.214	0.296
HB8	<i>Bacillus paramycoides</i> strain 3664	+	356	3.339	0.174
HC3	<i>Alishewanella jeotgali</i> KCTC 22429	+	358	0.616	0.702
HD3	<i>Franconibacter daqui</i> strain L17	+	360	1.848	0.08
HD4	<i>Enterobacter hormaechei</i> strain WG12L-2G-A	+	342	3.1017	0.12
HD5	<i>Shigella sonnei</i> strain 08BF03TD	+	355	2.52	0.04
HD6	<i>Enterobacteriaceae</i> bacterium v450	+	362	0.69	0.3
HE2	<i>Lysinibacillus boronitolerans</i>	+	359	1.47	0.26

strain Mix24					
HF2	<i>Bacillus cereus strain SPA1.1</i>	+	358	3.59	0.02
HF3	<i>Lysinibacillus macroides strain SKC-16</i>	+	358	2.53	0.1
HF4	<i>Lysinibacillus boronitolerans strain Mix24</i>	+	363	1.06	0.46
HF5	<i>Halotalea alkalilenta strain AW-7</i>	+	358	1.857	0.06
HR2	<i>Enterobacter cloacae strain UKME01</i>	+	357	0.75	0.24
HR3	<i>Enterobacteriaceae bacterium v450</i>	+	360	0.823	0.22

## DISCUSSION

The use of microbes for the manufacture of iron oxide nanoparticles (IONPs) offers several benefits in comparison with other techniques. Many microbes possess the capacity to gather and reduce metals, and this capability may be used to transform iron ions from metal salts into nanoparticles (Zúñiga-Miranda *et al.*, 2023). In the present study, the Gram-negative bacteria was more than Gram-positive bacteria. This result agree with study of Al Khafaji *et al.* (2023). Gram-negative bacteria were prevalent in HA, HC, HD, HR, and HB. Bacteria that produce lipase enzyme have been isolated from lipid-rich environments, and Gram-negative bacteria have a higher production rate than Gram-positive bacteria (Tarhriz *et al.*, 2011; Aktar *et al.*, 2021). *Pseudomonas* sp. can adapt to the presence of toxic compounds and their fluidizing properties by isomerization of this unsaturated fatty acids to their appropriate trans isomers. The degree of isomerization obviously depends on the toxicity and the concentration of membrane-affecting agents (Heipieper *et al.*, 2018). Gram-positive bacteria were more than Gram-negative bacteria in soil of HE, and HF, these results agree with the outcomes of Alshami *et al.* (2022) and Qays *et al.* (2023). The ability of *Bacillus* genus members to persist in diverse and extreme conditions is attributed to the development of protective endospores that can tolerate adverse environmental factors (Zammuto *et al.*, 2020).

*Halomonas*, *Rhizobium*, *Pseudomonas*, and *Bacillus* were isolated from oil refinery (Lukhele *et al.*, 2021). *Enterobacter ludwigii* (KWB3) was isolated from oil refinery effluent wastewater that have the ability to resist heavy metals and PAHs (Khatoun & Malik, 2019). In the present study, the isolates of *Stutzerimonas* sp. and *Alishewanella* sp. were dominated, and this result agrees with that of Salvà-Serra *et al.* (2023), who found that 23% of isolates are *S. balearica* in addition to the detection of other *Stutzerimonas* sp. from polluted environments with petroleum oil. Kumari and Chandra (2023) argued that *Stutzerimonas stutzeri* (LOBP-19) was most effective in environment contaminated with benzo[a]pyrene due to the presence of laccase, catechol

2,3-dioxygenase and peroxidase enzymes. *Alishewanella* displayed endurance to increased toxicity and showed proficiency in breaking down oils (Ren *et al.*, 2024).

According to nitrate reduction test, all isolates have the ability to reduce metal salts to nanoparticles. Bacteria have the capacity to detoxify and reduce the metal ions through the nitrate reductase enzyme or NADH-dependent reductase. Consequently, they employ this capability to synthesize metallic nanoparticles (Singh *et al.*, 2016; Alam *et al.*, 2020; Zakariya *et al.*, 2022b). In their study, Singh *et al.* (2016) discovered that the process of metal nanoparticle formation in *Bacillus licheniformis* was facilitated by the nitrate reductase enzyme. Fatemi *et al.* (2018) documented that the *B. cereus* strain *HMHI* has the ability to convert iron ions into iron nanoparticles.

The results of the IONP synthesis showed that the color of all mixtures (supernatant and  $\text{FeCl}_3 \cdot 6\text{H}_2\text{O}$ ) changed from pale yellow to brown or reddish brown, indicating the successful synthesis of IONPs. This observation aligns with the findings of Periyathambi *et al.* (2014) and Zakariya *et al.* (2022a). This was related to surface plasmon resonance SPR (Sharif *et al.*, 2023). In the aforementioned surface, the size and form of the synthesized NPs affect its peak position (Rasool & Hemalatha, 2017). The phenomenon of surface plasmon resonance is responsible for the hue shift. The collective electron oscillation in metal nanoparticles produces a Surface Plasmon Resonance (SPR) absorption band, which is responsible for the observed absorption in the range of 342–457nm (Alshami *et al.*, 2022). This range is consistent with the findings of Fani *et al.* (2018), Jubran *et al.* (2020) and Majeed *et al.* (2021). The reduction of ferric ions in solution is likely due to melanin-like pigments, which provide iron reductase activity that facilitates the absorption and incorporation of Fe ions (Jacob *et al.*, 2017).

Among the isolates, *Alishewanella jeotgali* KCTC 22429, *Leclercia adecarboxylata* strain V894, and *Lysinibacillus boronitolerans* strain Mix24 showed superior performance. The highest production rates were 0.702, 0.5, and 0.46g/l, respectively, as shown in Table (4). *Alishewanella jeotgali* KCTC 22429 was the most effective compared to the other isolates, which aligns with the results of Xia *et al.* (2016). *Leclercia adecarboxylata* can synthesize nanoparticles through interactions between proteins and metal salts (Abdelmoneim *et al.*, 2022). Additionally, Gurunathan *et al.* (2009) observed that proteins can produce nanoparticles via their unbound amine groups or cysteine residues.

## CONCLUSION

Twenty-two bacterial isolates were collected from five oil-contaminated sites in Basrah Governorate, southern Iraq. These bacteria belong to thirteen different genera, with nine isolates recorded in GenBank as new strains. All bacterial isolates possessed the nitrate reductase enzyme. The bacteria varied in their ability to reduce iron salts to

iron oxide nanoparticles (IONPs). The most effective isolate was *Alishewanella jeotgali* KCTC 22429, which produced 0.702g/ l of IONPs, with an absorption peak at 358nm.

## REFERENCES

- Abdelmoneim, H. M.; Taha, T. H. ; Elnouby; M. S. and AbuShady, H. M.** (2022). Extracellular biosynthesis, OVAT/statistical optimization, and characterization of silver nanoparticles (AgNPs) using *Leclercia adecarboxylata* THHM and its antimicrobial activity. *Microbial Cell Factories.*, 21(1), 277. <https://doi.org/10.1186/s12934-022-01998-9>.
- Abdul-Ameer, W. A.** (2019). Biodegradation and phytotoxicity of crude oil hydrocarbons in an agricultural soil. *Chilean journal of agricultural research.*, 79(2): 266-277. <http://dx.doi.org/10.4067/S0718-58392019000200266>.
- Ahmad, F. ; Salem-Bekhit, M. M. ; Khan, F. ; Alshehri, S. ; Khan, A., Ghoneim, M. M. and Elbagory, I.** (2022). Unique properties of surface-functionalized nanoparticles for bio-application: functionalization mechanisms and importance in application. *Nanomaterials*, 12(8), 1333. <http://dx.doi.org/10.3390/nano12081333>.
- Aktar, L. ; Moniruzzaman, M. ; Sakai, Y. and Saha, M. L.** (2021). Indigenous lipase producing bacteria for lipid-rich wastewater treatment. *Plant Tissue Culture and Biotechnology.*, 31(2): 135-142. <https://doi.org/10.3329/ptcb.v31i2.57341>.
- Al Khafaji, A. M. ; Almansoor, A. F. and Alyousif, N. A.** (2023). Isolation, screening and molecular identification of biofloculants–producing bacteria. *Biodiversitas Journal of Biological Diversity*, 24(8). <https://doi.org/10.13057/biodiv/d240822>
- Alam, H. ; Khatoon, N. ; Khan, M. A. ;Husain, S. A. ; Saravanan, M. and Sardar, M.** (2020). Synthesis of selenium nanoparticles using probiotic bacteria *Lactobacillus acidophilus* and their enhanced antimicrobial activity against resistant bacteria. *Journal of Cluster Science.*, 31:1003-1011. <https://doi.org/10.1007/s10876-019-01705-6>.
- Alhalili, Z.** (2023). Metal oxides nanoparticles: general structural description, chemical, physical, and biological synthesis methods, role in pesticides and heavy metal removal through wastewater treatment. *Molecules*, 28(7), 3086. <https://doi.org/10.3390/molecules28073086>
- Almutairi, H. H.** (2024). Microbial communities in petroleum refinery effluents and their complex functions. *Saudi Journal of Biological Sciences*, 104008. <https://doi.org/10.1016/j.sjbs.2024.104008>.
- Alshami, H. G. A. ; Al-Tamimi, W. H. and Hateet, R. R.** (2022). Screening for extracellular synthesis of silver nanoparticles by bacteria isolated from Al-Halfaya oil

field reservoirs in Missan province, Iraq. *Biodiversitas Journal of Biological Diversity*, 23(7). <https://doi.org/10.13057/biodiv/d230720>.

**Bhusal , A. and Muriana P.M.** (2021). Isolation and characterization of nitrate reducing bacteria for conversion of vegetable-derived nitrate to ‘natural nitrite. *Appl Microbiol.*, 1 (1): 11-23. <https://doi.org/10.3390/applmicrobiol1010002>.

**Crespo, K. A. ; Baronetti, J. L. ; Quinteros, M. A. ; Páez, P. L. and Paraje, M. G.** (2017). Intra-and extracellular biosynthesis and characterization of iron nanoparticles from prokaryotic microorganisms with anticoagulant activity. *Pharmaceutical research.*, 34: 591-598. <https://doi.org/10.1007/s11095-016-2084-0>.

**Elfeky, A. S. ;Salem, S. S. ; Elzaref, A. S. ; Owda, M. E. ;Eladawy, H. A. ; Saeed, A. M. and Fouda, A.** (2020). Multifunctional cellulose nanocrystal/metal oxide hybrid, photo-degradation, antibacterial and larvicidal activities. *Carbohydrate polymers*, 230, 115711. <https://doi.org/10.1016/j.carbpol.2019.115711>.

**Ene, V. L. ;Neacsu, I. A. ; Oprea, O. V. ; Surdu, V. A. ; Trusca, R. D. ; Ficai, A. N. and Andronescu, E. C.** (2020). Single Step Synthesis of Glutamic/tartaric Acid stabilized Fe<sub>3</sub>O<sub>4</sub> Nanoparticles for Targeted Delivery Systems. *Rev. Chim.*, 71: 230-238. <https://doi.org/10.37358/rc.20.2.7920>.

**Fani, M. ; Ghandehari, F. and Rezaee, M.** (2018). Biosynthesis of iron oxide nanoparticles by cytoplasmic extract of bacteria *lactobacillus fermentum*. *J Med Chem Sci.*, 1(2): 28-30. <https://doi.org/10.26655/jmchemsci.2018.9.2>.

**Fatemi, M. ; Mollania, N. ; Momeni-Moghaddam, M. and Sadeghifar, F.** (2018). Extracellular biosynthesis of magnetic iron oxide nanoparticles by *Bacillus cereus* strain HMH1: Characterization and in vitro cytotoxicity analysis on MCF-7 and 3T3 cell lines. *Journal of biotechnology.*, 270: 1-11. <https://doi.org/10.1016/j.jbiotec.2018.01.021>

**Gorobets, O.; Gorobets, S. and Koralewski, M.** (2017). Physiological origin of biogenic magnetic nanoparticles in health and disease: from bacteria to humans. *International journal of nanomedicine.*, 4371-4395. <https://doi.org/10.2147/IJN.S130565>.

**Gurunathan, S. ; Kalishwaralal, K. ; Vaidyanathan, R. ; Venkataraman, D. ; Pandian, S. R. K. ; Muniyandi, J. and Eom, S. H.** (2009). Biosynthesis, purification and characterization of silver nanoparticles using *Escherichia coli*. *Colloids and Surfaces B: Biointerfaces.*, 74(1):328-335. <https://doi.org/10.1016/j.colsurfb.2009.07.048>.

**Hassan D. F. and Mahmood M.** (2019). Biosynthesis of iron oxide nanoparticles using *Escherichia coli*, *Iraqi Journal of Science.*, 66: 453-459. <https://doi.org/10.24996/ijcs.2019.60.3.5>.

**Heipieper, H. J. ; Fischer, J. and Meinhardt, F.** (2018). Cis–trans isomerase of unsaturated fatty acids: An immediate bacterial adaptive mechanism to cope with

emerging membrane perturbation caused by toxic hydrocarbons. *Cellular Ecophysiology of Microbe: Hydrocarbon and Lipid Interactions.*, 385-395. [https://doi.org/10.1007/978-3-540-77587-4\\_112](https://doi.org/10.1007/978-3-540-77587-4_112).

**Jacob, P. J. ; Masarudin, M. J. ; Hussein, M. Z. and Rahim, R. A.** (2017). Facile aerobic construction of iron based ferromagnetic nanostructures by a novel microbial nanofactory isolated from tropical freshwater wetlands. *Microbial cell factories.*, 16:1-14. <https://doi.org/10.1186/s12934-017-0789-3>.

**Jubran, A. S. ;Al-Zamely, O. M. and Al-Ammar, M. H.** (2020). A study of iron oxide nanoparticles synthesis by using bacteria. *Int. J. Pharm. Qual. Assur.*, 11(01): 01-08. <https://doi.org/10.25258/ijpqa.11.1.13>.

**Khatoon, K. and Malik, A.** (2019). Screening of polycyclic aromatic hydrocarbon degrading bacterial isolates from oil refinery wastewater and detection of conjugative plasmids in polycyclic aromatic hydrocarbon tolerant and multi-metal resistant bacteria. *Heliyon.*, 5(10). <https://doi.org/10.1016/j.heliyon.2019.e02742>.

**Kumar, S. ; Stecher, G. ;Li, M., Knyaz, C. and Tamura, K.** (2018). MEGA X: molecular evolutionary genetics analysis across computing platforms. *Molecular biology and evolution.*, 35(6):1547-1549. <https://doi.org/10.1093/molbev/msy096>.

**Kumari, B. and Chandra, R.** (2023). Benzo [a] pyrene degradation from hydrocarbon-contaminated soil and their degrading metabolites by *Stutzerimonas stutzeri* (LOBP-19A). *Waste Management Bulletin.*, 1(3):115-127. <https://doi.org/10.1016/j.wmb.2023.07.006>

**Lukhele, T. ; Nyoni, H. ; Mamba, B. B. and Msagati, T. A. M.** (2021). Unraveling bacterial diversity in oil refinery effluents. *Archives of Microbiology.*, 203: 1231-1240. <https://doi.org/10.1007/s00203-020-02062-z>.

**Majeed, S. ; Danish, M. ; Mohamad Ibrahim, M. N. ; Sekeri, S. H. ; Ansari, M. T. ; Nanda, A. and Ahmad, G.** (2021). Bacteria mediated synthesis of iron oxide nanoparticles and their antibacterial, antioxidant, cytocompatibility properties. *Journal of Cluster Science.*, 32: 1083-1094. <https://doi.org/10.1007/s10876-020-01876-7>.

**Miyoshi, T. ; Iwatsuki, T. and Naganuma, T.** (2005). Phylogenetic characterization of 16S rRNA gene clones from deep-groundwater microorganisms that pass through 0.2-micrometer-pore-size filters. *Applied and environmental microbiology*, 71(2):1084-1088. <https://doi.org/10.1128/AEM.71.2.1084-1088.2005>.

**Mukherjee, P.** (2017). *Stenotrophomonas* and *Microbacterium*: Mediated biogenesis of copper, silver and iron nanoparticles—Proteomic insights and antibacterial properties



versus biofilm formation. *Journal of cluster science.*, 28: 331-358. <https://doi.org/10.1007/s10876-016-1097-5>.

**Nadeem, M. ;Khan, R. ;Shah, N. ; Bangash, I. R. ; Abbasi, B. H. ; Hano, C. and Celli, J.** (2021). A review of microbial mediated iron nanoparticles (IONPs) and its biomedical applications. *Nanomaterials.*, 12(1), 130. <https://doi.org/10.3390/nano12010130>.

**Pannekens, M. ; Kroll, L. ; Müller, H. ; Mbow, F. T. and Meckenstock, R. U.** (2019). Oil reservoirs, an exceptional habitat for microorganisms. *New Biotechnology.*, 49: 1-9. <https://doi.org/10.1016/j.nbt.2018.11.006>.

**Park, T. J. ; Lee, K. G. and Lee, S. Y.** (2016). Advances in microbial biosynthesis of metal nanoparticles. *Applied microbiology and biotechnology.*, 100: 521-534. <https://doi.org/10.1007/s00253-015-6904-7>.

**Periyathambi, P. ; Vedakumari, W. S. ; Bojja, S. ; Kumar, S. B. and Sastry, T. P.** (2014). Green biosynthesis and characterization of fibrin functionalized iron oxide nanoparticles with MRI sensitivity and increased cellular internalization. *Materials Chemistry and Physics.*, 148(3), 1212-1220. <https://doi.org/10.1016/j.matchemphys.2014.09.050>.

**Qays, H. ; Almansoor, A. F. and Al-Baldawi, I. A.** (2023). Interaction Between *Typha domingensis* and Bacteria *Bacillus sp.* to Treatment of Wastewater Polluted by Kerosene. In *IOP Conference Series: Earth and Environmental Science* (Vol. 1215, No. 1, p. 012047). IOP Publishing. <https://doi.org/10.1088/1755-1315/1215/1/012047>.

**Rabani, G. ; Dilshad, M. ;Sohail, A. ; Salman, A. ; Ibrahim, S. ; Zafar, I. and Arshad, H. M.** (2023). Extracellular synthesis of iron oxide nanoparticles using an extract of *Bacillus circulans*: characterization and in vitro antioxidant activity. *Journal of Chemistry.*, 2023(1), 4659034. <https://doi.org/10.1155/2023/4659034>.

**Rasool, U. and Hemalatha, S. J. M. L.** (2017). Marine endophytic actinomycetes assisted synthesis of copper nanoparticles (CuNPs): characterization and antibacterial efficacy against human pathogens. *Materials Letters*, 194, 176-180. <https://doi.org/10.1016/j.matlet.2017.02.055>

**Ren, H. ; Deng, Y. ; Zhao, D. ; Jin, W. ; Xie, G. ; Peng, B. and Wang, B.** (2024). Structures and diversities of bacterial communities in oil-contaminated soil at shale gas well site assessed by high-throughput sequencing. *Environmental Science and Pollution Research.*, 31(7), 10766-10784. <https://doi.org/10.1007/s11356-023-31344-4>.

**Salem, D. M. ; Ismail, M. M. and Aly-Eldeen, M. A.** (2019). Biogenic synthesis and antimicrobial potency of iron oxide (Fe<sub>3</sub>O<sub>4</sub>) nanoparticles using algae harvested from the

Mediterranean Sea, Egypt. The Egyptian Journal of Aquatic Research., 45(3), 197-204. <https://doi.org/10.1016/j.ejar.2019.07.002>.

**Salvà-Serra, F. ; Pérez-Pantoja, D. ; Donoso, R. A. ; Jaén-Luchoro, D. ; Fernández-Juárez, V. ; Engström-Jakobsson, H. and Bennasar-Figueras, A.** (2023). Comparative genomics of *Stutzerimonas balearica* (*Pseudomonas balearica*): diversity, habitats, and biodegradation of aromatic compounds. *Frontiers in Microbiology.*, 14, 1159176. <https://doi.org/10.3389/fmicb.2023.1159176>.

**Samrot, A. V. ; Sahithya, C. S. ; Selvarani, J. ; Purayil, S. K. and Ponnaiah, P.** (2021). A review on synthesis, characterization and potential biological applications of superparamagnetic iron oxide nanoparticles. *Current Research in Green and Sustainable Chemistry.*, 4, 100042. <https://doi.org/10.1016/j.crgsc.2020.100042>.

**Shafey, A. M. E.** (2020). Green synthesis of metal and metal oxide nanoparticles from plant leaf extracts and their applications: A review. *Green Processing and Synthesis.*, 9(1): 304-339. <https://doi.org/10.1515/gps-2020-0031>.

**Sharif, M. S. ; Hameed, H. ; Waheed, A. ; Tariq, M. ; Afreen, A. ; Kamal, A. and Zaman, W.** (2023). Biofabrication of Fe<sub>3</sub>O<sub>4</sub> nanoparticles from *Spirogyra hyalina* and *Ajuga bracteosa* and their antibacterial applications. *Molecules.*, 28(8), 3403. <https://doi.org/10.3390/molecules28083403>

**Singh ,H. ; Du ,J.; Singh, P. and Yi TH.** (2018). Extracellular synthesis of silver nanoparticles by *Pseudomonas sp.* THG-LS1.4 and their antimicrobial application. *J Pharm Anal.*, 8 (4): 258-264. <https://doi.org/10.1016/j.jpha.2018.04.004>.

**Singh, P. ; Kim, Y. J. ; Zhang, D. and Yang, D. C.** (2016). Biological synthesis of nanoparticles from plants and microorganisms. *Trends in biotechnology.*, 34(7), 588-599. <https://doi.org/10.1016/j.tibtech.2016.02.00>.

**Sundaram, P. A. ; Augustine, R. and Kannan, M.** (2012). Extracellular biosynthesis of iron oxide nanoparticles by *Bacillus subtilis* strains isolated from rhizosphere soil. *Biotechnology and bioprocess engineering.*, 17, 835-840. <https://doi.org/10.1007/s12257-011-0582-9>.

**Tarhriz, V. ; Mohammadzadeh, F. ; Hejazi, M. S. ; Nematzadeh, G. and Rahimi, E.** (2011). Isolation and characterization of some aquatic bacteria from Qurug? l lake in Azerbaijan under aerobic conditions. *Advances in Environmental Biology.*, 5(10), 3173-3178.

**Üstün, E. ; Önbaşı, S. C. ; Çelik, S. K. ; Ayvaz, M. Ç. and Şahin, N.** (2022). Green synthesis of iron oxide nanoparticles by using *Ficus carica* leaf extract and its antioxidant activity. *Biointerface Res. Appl. Chem.*, 12(2), 2108-2116. <https://doi.org/10.33263/BRIAC122.21082116>.

**Valentina ,Y.** (2022). Optimisation of reactant concentration in biosynthesis of silver nanoparticles using pathogenic bacteria isolated from clinical sources and their characterisation: a recent study. *Innov Microbiol Biotechnol.*, 3 (1): 45-55. <https://doi.org/10.9734/bpi/imb/v3/173a>.

**Xia, X. ; Li, J. ; Liao, S. ; Zhou, G. ; Wang, H. ; Li, L. and Wang, G.** (2016). Draft genomic sequence of a chromate-and sulfate-reducing *Alishewanella* strain with the ability to bioremediate Cr and Cd contamination. *Standards in genomic sciences.*, 11, 1-8. <https://doi.org/10.1186/s40793-016-0169-3>.

**Yew, Y. P. ; Shameli, K. ; Miyake, M. ; Khairudin, N. B. B. A. ; Mohamad, S. E. B. ; Naiki, T. and Lee, K. X.** (2020). Green biosynthesis of superparamagnetic magnetite Fe<sub>3</sub>O<sub>4</sub> nanoparticles and biomedical applications in targeted anticancer drug delivery system: A review. *Arabian Journal of Chemistry.*, 13(1), 2287-2308. <https://doi.org/10.1016/j.arabjc.2018.04.013>.

**Zakariya, N. A. ; Jusof, W. H. W. and Majeed, S.** (2022)a. Green approach for iron oxide nanoparticles synthesis: application in antimicrobial and anticancer-an updated review. *Karbala International Journal of Modern Science.*, 8(3), 421-437. <https://doi.org/10.33640/2405-609X.3256>.

**Zakariya, N. A. ; Majeed, S. and Jusof, W. H. W.** (2022)b. Investigation of antioxidant and antibacterial activity of iron oxide nanoparticles (IONPS) synthesized from the aqueous extract of *Penicillium* spp. *Sensors International.*, 3, 100164. <https://doi.org/10.1016/j.sintl.2022.100164>.

**Zammuto, V. ;Rizzo, M. G. ; De Plano, L. M. ; Franco, D.; Guglielmino, S. ; Caccamo, M. T. and Gugliandolo, C.** (2020). Effects of heavy ion particle irradiation on spore germination of *Bacillus* spp. from extremely hot and cold environments. *Life.*, 10(11), 264. <https://doi.org/10.3390/life10110264>.

**Zúñiga-Miranda, J. ; Guerra, J. ; Mueller, A. ; Mayorga-Ramos, A. ; Carrera-Pacheco, S. E. ;Barba-Ostria, C. and Guamán, L. P.** (2023). Iron oxide nanoparticles: green synthesis and their antimicrobial activity. *Nanomaterials.*, 13(22), 2919. <https://doi.org/10.3390/nano13222919>.